A New Approach to Robust and Fault Tolerant Control[1)]

Kemin Zhou

(*Department of Electrical and Computer Engineering, Louisiana State University, Baton Rouge, LA* 70803 *U.S.A.*)

(E-mail: kemin@ece.lsu.edu)

Abstract In this paper, we shall summarize a new approach to robust and fault tolerant control proposed recently by the author. This approach is based on a variation of all controller parametrization. This robust and fault-tolerant control design consists of two parts: a nominal performance controller and a robustness controller, and works in such a way that when a component (sensor, actuator, etc.) failure is detected, the controller structure is reconfigured by adding a robustness loop to compensate the fault. We shall illustrate how this strategy works under various situations.

Key words Robustness, robust performance, design tradeoff, fault tolerant control, generalized internal model control

1 Introduction

It is commonly known in the control community that there are intrinsic tradeoffs between achievable performance and robustness for a given control architecture, see for example[1∼5] for some detailed analysis and discussions. In other words, in order to achieve certain performance, one must sacrifices some robustness properties of the control systems and vise versa once the control architecture is chosen. For example, a high performance controller designed for a nominal model may have very little robustness against the model uncertainties and external disturbances. For this reason, worst-case robust control design techniques such as H_∞ control, L_1 control, μ synthesis, etc., have gained popularity in the last twenty years or so, see for example[4∼8], and references therein. Unfortunately, it is well recognized in the robust control community that the robustness of a closed-loop system design is usually achieved at the expense of performance. In particular, it is well known that robust control design techniques such as H_∞ optimization, L_1 optimization, and μ synthesis usually result in controllers that are robust to model uncertainties and external disturbances but may have very poor nominal performance. This is not hard to understand since most robust control design techniques are based on the worst possible scenarios that may never occur in a particular control system. Thus such controllers are not desirable in many applications. Nevertheless, the ability to be able to control the system under the worst-case scenario is also very important in many applications and hence it is desirable to have design techniques that can achieve the same level of robustness when there are model uncertainties and external disturbances while at the same time perform well when there is no or little model uncertainties and external disturbances. The control architecture proposed by this author in [9], which is called Generalized Internal Model Control (GIMC), seems to be a good candidate for achieving this objective. In other words, the tradeoffs between robustness and performance in a feedback control system depend very much on the control architecture. See [10 ∼ 12] for some applications.

A problem closely related to the above tradeoff is to keep good performance in the event of sensor/actuator failures that are crucial in many applications, especially if costly equipments are controlled. One way of synthesizing fault-tolerant controllers is by appealing to H_∞ robust design techniques[5,13]. Unfortunately, as we have discussed earlier, the standard H_∞ based robust control design is based on the worst case scenario which may never occur and it is not surprising to see that such a control system does not perform very well even though it is robust to model uncertainties and sensor/actuator faults.

It is our intention in this paper to demonstrate this new design technique through two simple examples so that application engineers may make appropriate decisions in their applications as what the most effective techniques may be applied.

The paper is organized as follows. Section 2 introduces the GIMC architecture. Section 3 shows a robust control example using the GIMC control design technique and demonstrates its effectiveness.

1) Supported in part by grants from NASA and the Louisiana Board of Regents
Received December 17, 2003; in revised form October 25, 2004

Copyright © 2005 by Editorial Office of Acta Automatica Sinica. All rights reserved.

Section 4 shows how the method can be used to fault tolerant control of a gyroscope system. Some concluding remarks are given in Section 5.

2 A new control structure for robust and fault tolerant control

Consider a standard feedback configuration shown in Fig. 1 where $\tilde{G}$ is a linear time invariant plant and K is a linear time invariant controller. It is well understood that the model $\tilde{G}$ is in general not perfectly known. What one actually knows is a nominal model G. Now assume that K_0 is a stabilizing controller for the nominal plant G and assume G and K_0 have the following stable coprime factorizations

$$K_0 = \tilde{V}^{-1}\tilde{U}, \quad G = \tilde{M}^{-1}\tilde{N}$$

Then it is well known[4,5] that every stabilizing controller for G can be written in the following form:

$$K = (\tilde{V} - Q\tilde{N})^{-1}(\tilde{U} + Q\tilde{M})$$

for some $Q \in H_\infty$ such that $\det(\tilde{V}(\infty) - Q(\infty)\tilde{N}(\infty)) \neq 0$.

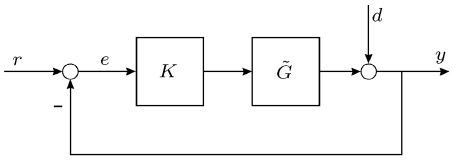

Fig. 1 Standard feedback configuration

It is proposed in [9] that this controller can be implemented as shown in Fig. 2. This controller architecture is called the Generalized Internal Model Control (GIMC) in [9] due to the similarity with the well-known Internal Model Control (IMC), see [14]. Note that the feedback diagram in Fig. 2 is not equivalent to the diagram in Fig. 1 since the reference signal r enters into the system from a different location. Nevertheless, the internal stability of the system is not changed since the transfer function from y to u is $-K$ and is not changed. Thus this controller implementation also stabilizes internally the feedback system with plant G for any $Q \in H_\infty$ such that $\det(\tilde{V}(\infty) - Q(\infty)\tilde{N}(\infty)) \neq 0$.

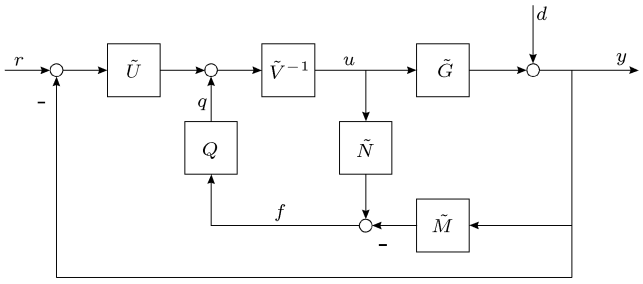

Fig. 2 Generalized Internal Model Control Structure

The distinct feature of this controller implementation is that the inner loop feedback signal f is always zero, *i.e.*, $f = 0$, if there is no model uncertainties (*i.e.*, $\tilde{G} = G$), external disturbances or faults and then the control system will be solely controlled by the high performance controller $K_0 = \tilde{V}^{-1}\tilde{U}$. On the other hand, the controller Q in the inner loop will only be active when $f \neq 0$, *i.e.*, there are either model uncertainties or external disturbances or sensor/actuator faults. Moreover, the strength of the signal q depends on the size of the model uncertainties, the size of the disturbances, and the extents of the faults. Hence Q can be designed to robustify the feedback systems. Thus this controller design architecture has a clear separation between performance and robustness.

In contrast, we note that the standard implementation of K in Fig. 1 is equivalent to the five block implementation shown in Fig. 3. It is clear in Fig. 3 that the reference signal r is always processed by $\tilde{M}$ and Q so that q is generally nonzero even if there is no uncertainty or sensor/actuator faults. It is thus impossible to separate the tracking performance and robustness in the standard implementation.

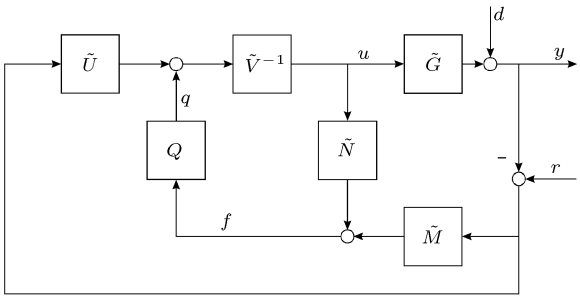

Fig. 3 Five block implementation of the standard feedback control

Controller Design 1. A high performance robust system can be designed in two steps: (a) Design $K_0 = \tilde{V}^{-1}\tilde{U}$ to satisfy the system performance specifications with a nominal plant model G; (b) Design a stable Q to satisfy the system robustness requirements. Note that the controller Q will not affect the system nominal performance.

Alternatively, we can find Q from a nominal high performance controller K_0 and a robust controller K.

Controller Design 2. Suppose one has already designed a good nominal controller K_0 and one has also designed a robust controller K for the same system. Then a stable Q can be constructed as

$$Q = \tilde{V}(K - K_0)(\tilde{N}K + \tilde{M})^{-1}$$

In the case when $\tilde{U}$ (or equivalently K_0) is strictly minimum phase, then without loss of generality, we can take $Q = \tilde{U}\hat{Q}$ for some stable $\hat{Q}$. Then the controller can be written as

$$K = (I - K_0\hat{Q}\tilde{N})^{-1}(K_0 + K_0\hat{Q}\tilde{M})$$

and the GIMC structure becomes the one shown in Fig. 4.

If in addition to K_0 being strictly minimum phase, G is also stable, then GIMC can take the form shown in Fig. 5.

The above control structure also provides a systematic method for fault tolerant control design. Note that $f(s) = \tilde{N}(s)u(s) - \tilde{M}(s)y(s)$ is the filtered error between the estimated output and the true output of the system (residual signal)[13]. This signal contains valuable information in case of a system components/sensors/actuators failure. Consequently, in order to have the exact nominal performance in case of no-failure, f could be monitored to detect a sensor or actuator failure and then activate the robustness loop, *i.e.* switch on the signal q. Thus, the GIMC structure can also be implemented as shown in Fig.6. Note that in this case Q can be a set of controllers corresponding to specific situations. This will improve the performance of the overall GIMC structure, since there is no degradation of nominal performance in order to improve robustness.

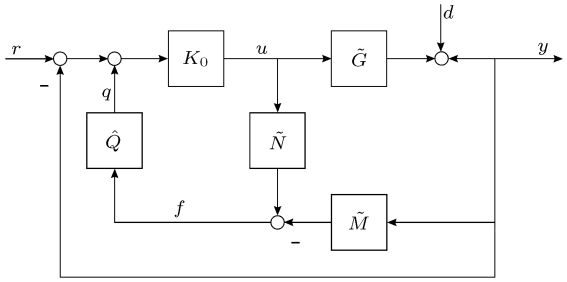

Fig. 4 An alternative GIMC implementation

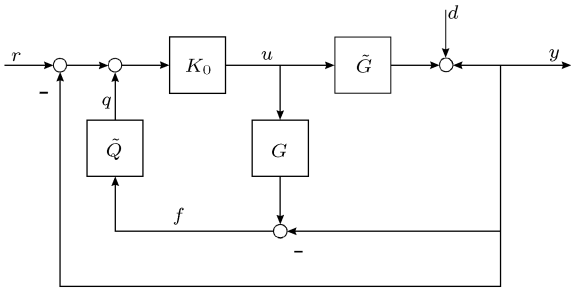

Fig. 5 GIMC when K_0 minimum phase and G stable

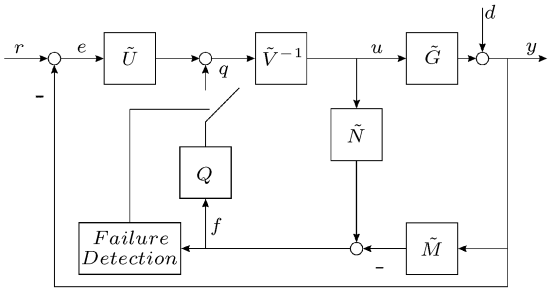

Fig. 6 GIMC structure with failure detector

We shall illustrate the above design philosophy with two examples in the subsequent sections.

3 A robust control example

To demonstrate the effectiveness of the GIMC architecture, we shall take a simple example from *μ-Analysis and Synthesis Toolbox*[6]. The nominal plant is given by

$$G = \frac{1}{s-1}$$

The true plant is known to be in a multiplicative set

$$\mathcal{M}(G, W_u) := \{G(1 + \Delta W_u) : \max_{\omega} |\Delta(j\omega)| \leqslant 1\}$$

with $W_u = \dfrac{\frac{1}{4}(\frac{1}{2}s + 1)}{\frac{1}{32}s + 1}$ and Δ can be any transfer function such that $G(1+\Delta W_u)$ and G have the same number of unstable poles. The block diagram of this control system is shown in Fig. 7.

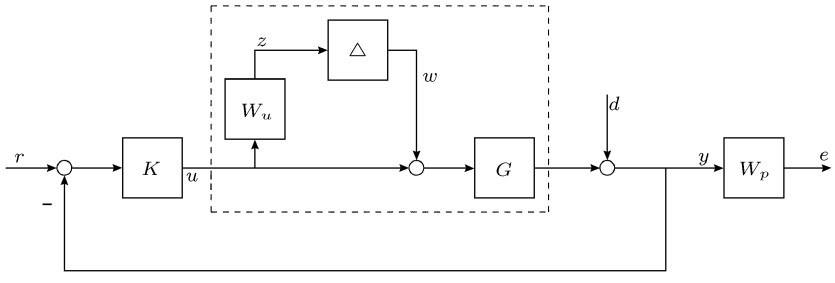

Fig. 7 Uncertain feedback control system

The feedback system can be put in a linear fractional transformation (LFT) form as shown in Fig. 8, with $P = \begin{bmatrix} 0 & 0 & W_u \\ W_pG & W_p & W_pG \\ G & I & G \end{bmatrix}$.

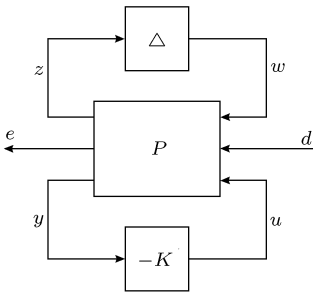

Fig. 8 LFT form of the feedback system

As stated in [6], the performance objective of this control system is to keep the closed-loop system stable and have output disturbance rejection up to 0.6 rad/sec, with at least 100:1 disturbance rejection at DC for all possible models in the set.

The design objective can be approximately represented as a weighted H_∞ norm constraint on the sensitivity function T_{ed}:

$$\|T_{ed}\|_\infty = \left\| \frac{W_p}{1+\tilde{G}K} \right\|_\infty \leqslant 1$$

for all $\tilde{G} \in \mathcal{M}(G, W_u)$ with the weighting function

$$W_p = \frac{\frac{1}{4}s + 0.6}{s + 0.006}$$

Let M be the transfer matrix from (w, d) to (z, e),

$$\begin{bmatrix} z \\ e \end{bmatrix} = M(s) \begin{bmatrix} w \\ d \end{bmatrix} = \begin{bmatrix} M_{11} & M_{12} \\ M_{21} & M_{22} \end{bmatrix} \begin{bmatrix} w \\ d \end{bmatrix}$$

Then the nominal performance (*i.e.*, when $\Delta = 0$) can be evaluated by the transfer function

$$T_{ed}^0 := T_{ed}|_{\Delta=0} = M_{22} = \frac{W_p}{1+GK}$$

and the robust stability margin can be evaluated by the transfer function

$$T_{zw} = M_{11} = \frac{W_uGK}{1+GK}.$$

Finally, the robust performance condition

$$\|T_{ed}\|_\infty = \left\| \frac{W_p}{1+\tilde{G}K} \right\|_\infty \leqslant 1$$

is satisfied if and only if the structured singular value

$$\mu_{\Delta_P}(M(j\omega)) \leqslant 1, \quad \forall\omega$$

where $\Delta_P = \mathrm{diag}(\Delta, \Delta_f)$.

Two PI controllers are designed in [6] for this uncertain system

$$K_1 = \frac{10(0.9s+1)}{s}, \quad K_2 = \frac{2.8s+1}{s}$$

The frequency responses of T_{ed}^0 for both controllers are shown in Fig. 9 and it is clear that the nominal performance criteria are satisfied by both controllers since $|T_{ed}^0(j\omega)| < 1$ for all frequencies. Moreover,

the plot also shows that K_1 has much better nominal performance than K_2 does. Similarly, the frequency responses of T_{zw} shown in Fig. 10 indicate that the robust stability condition, $\|T_{zw}\|_\infty < 1$, is satisfied by both controllers with K_2 having much large robust stability margin than K_1 does.

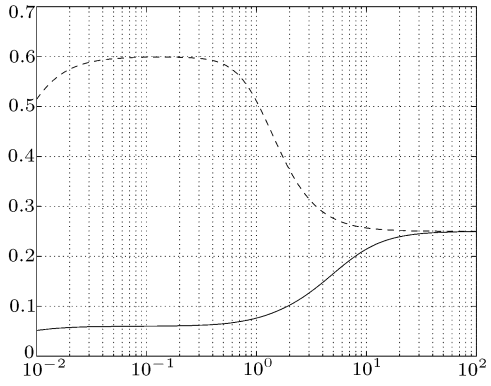

Fig. 9 Frequency responses of T_{ed}^0 for nominal performance: K_1 (solid) and K_2 (dashed)

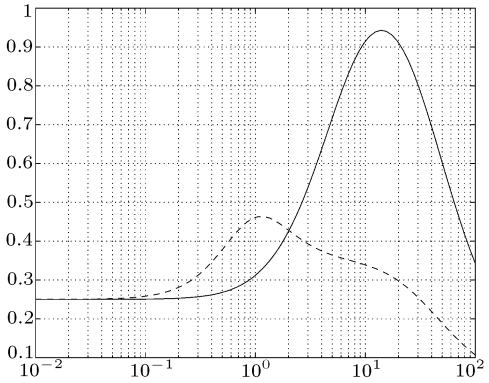

Fig. 10 Frequency responses of T_{zw} for robust stability: K_1 (solid) and K_2 (dashed)

On the other hand, the structured singular value plots in Fig. 11 show that the robust performance is satisfied with K_2 but is not satisfied with K_1.

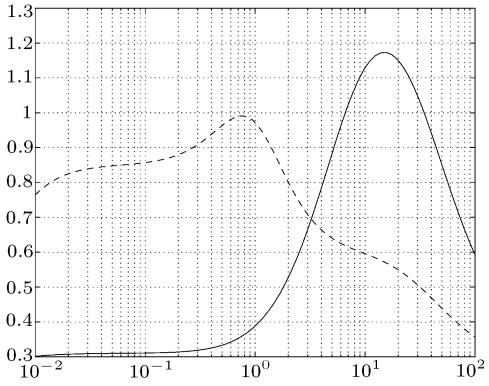

Fig. 11 Frequency responses of $\mu_{\Delta_P}(M(j\omega))$ for robust performance: K_1 (solid) and K_2 (dashed)

To evaluate the time domain behavior of the control system with both controllers, ten plants including the nominal and two "worst-case" plants in the set $\mathcal{M}(G, W_u)$ are used for performance evaluation in [6] and they are given by

$$G = \frac{1}{s-1},\ G_1 = \frac{1}{s-1}\frac{6.1}{s+6.1},\ G_2 = \frac{1.425}{s-1.425},\ G_3 = \frac{0.67}{s-0.67},\ G_4 = \frac{1}{s-1}\frac{-0.07s+1}{0.07s+1},$$

$$G_5 = \frac{1}{s-1}\frac{70^2}{s^2+2\times 0.15\times 70s+70^2},\ G_6 = \frac{1}{s-1}\frac{70^2}{s^2+2\times 5.6\times 70s+70^2},\ G_7 = \frac{1}{s-1}\left(\frac{50}{s+50}\right)^6,$$

$$G_{wc1} = \frac{1}{s-1}\frac{-2.9621(s-9.837)(s+0.76892)}{(s+32)(s+0.56119)},\ G_{wc2} = \frac{1}{s-1}\frac{s^2+3.6722s+34.848}{(s+7.2408)(s+32)}$$

The step responses of the closed-loop system with K_1 and K_2 implemented as in Fig. 1 are shown respectively in Fig. 12 and Fig. 13.

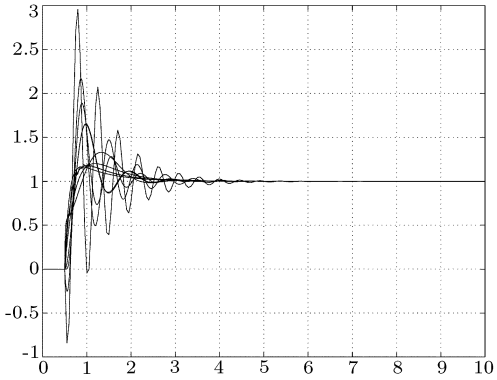

Fig. 12 Step response with K_1 and various plants for standard feedback implementation

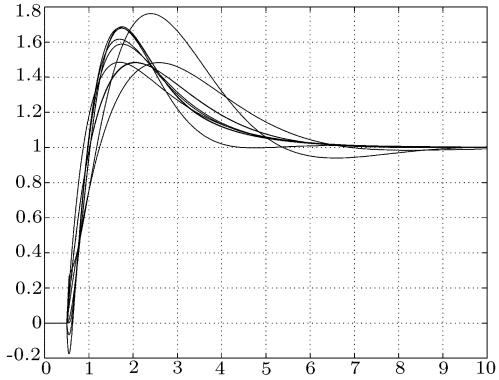

Fig. 13 Step response with K_2 and various plants for standard feedback implementation

It is clear from the simulations that controller K_1 gives very good and fast response for the nominal system but it performs very badly for some perturbed plants. On the other hand, controller K_2 shows a very robust performance with respect to model uncertainties but the responses are very slow and the closed-loop system performs poorly in the nominal case as well as in the perturbed case.

From the above analysis, it is very desirable to have a controller that will take advantages of good performance of K_1 in the nominal case and good robustness of K_2 in the perturbed cases. The GIMC architecture is a good candidate for achieving this objective.

Let $G = \tilde{N}/\tilde{M}$ be a stable factorization with

$$\tilde{N} = \frac{1}{s+1}, \quad \tilde{M} = \frac{s-1}{s+1}$$

Then it is easy to show that

$$K_2 = \frac{K_1(1+\hat{Q}\tilde{M})}{1-K_1\hat{Q}\tilde{N}}$$

with

$$\hat{Q}(s) = -\frac{0.1s(6.2s+1)(s+1)}{(0.9s+1)(s^2+1.8s+1)}$$

Hence the controller K_2 can be implemented using a GIMC structure as shown in Fig. 14. Note that the transfer function from y to u is $-K_2$. Thus the robustness properties of the closed-loop system are the same as the controller K_2 is implemented in the standard feedback framework.

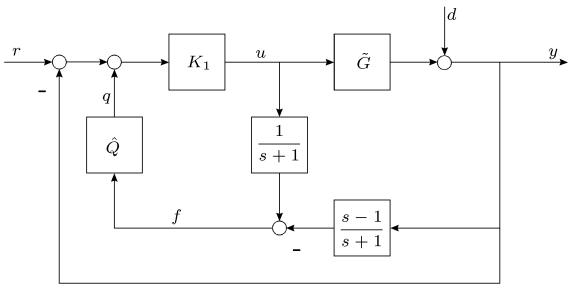

Fig. 14 GIMC implementation of K_2

The step responses of the nominal system with K_1, K_2, and the GIMC implementation are shown in Fig. 15. The step responses show clearly that the control system with K_1 and GIMC have the same nominal responses and are much better than that due to K_2. Fig. 16 shows the step responses of the

closed-loop system with the nominal model (G) as well as various perturbed models ($G_1, \ldots, G_7$, G_{wc1}, and G_{wc2}) when K_2 is implemented using the GIMC structure as shown in Fig. 14.

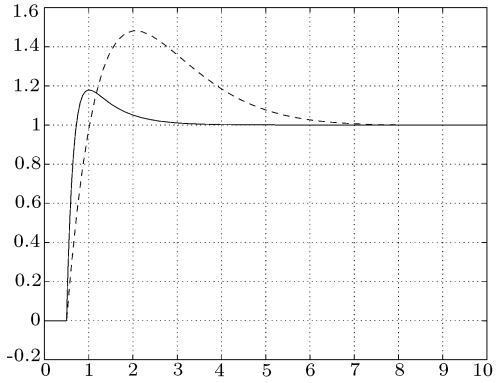

Fig. 15 Step responses of the nominal G: K_1 (solid), K_2 (dashed), GIMC (solid)

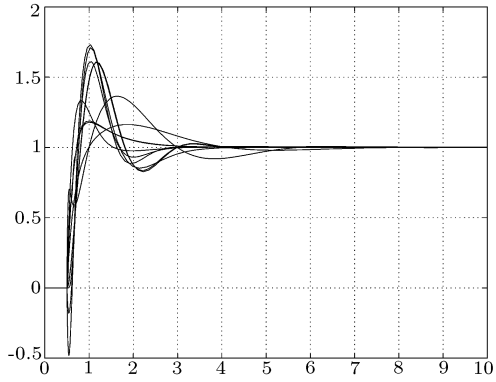

Fig. 16 Step responses of the closed-loop system with K_2 implemented using the GIMC structure under various perturbations

For comparison, the step responses for the "worst-case" plants with the controller K_1, K_2, and the GIMC implementation of K_2 are shown in Fig. 17 and 18. It is clear from the simulations that the GIMC implementation delivers good nominal response as well as superb robust performance.

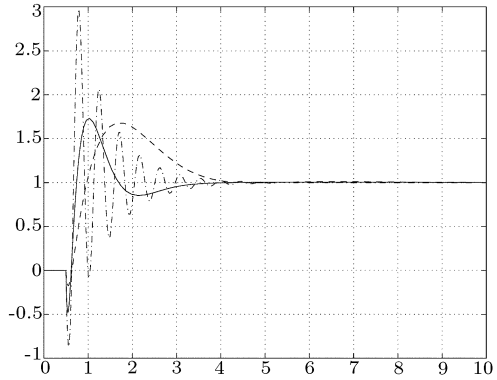

Fig. 17 Step responses of G_{wc2}: K_1 (dash-dot), K_2 (dashed), and GIMC (solid)

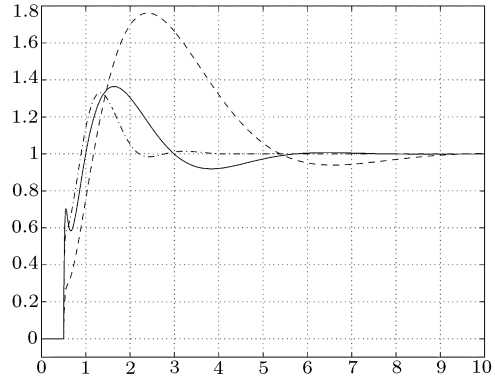

Fig. 18 Step responses of G_{wc2}: K_1 (dash-dot), K_2 (dashed), and GIMC (solid)

4 A fault tolerant control example

The fault tolerant structure will now be tested in a MIMO gyroscope experiment. This design example is discussed in detail in [11]. The plant, shown in Fig. 19, consists of a high inertia brass rotor suspended in an assembly with four angular degrees of freedom.

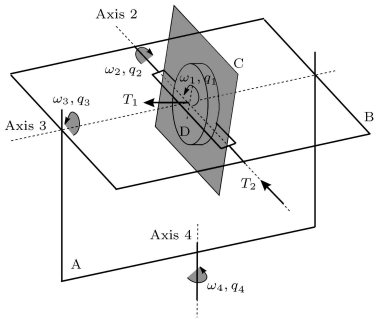

Fig. 19 A gyroscope system

Here we shall consider a special case where the gimbal Axis 3 is locked so that bodies A and B become one rigid body. The plant has all poles on the imaginary axis. Consequently, a high-gain observer-based controller is designed so that it has a fairly fast response with a small overshoot while keeping the controlling voltage between the limits of the saturation. In the next step of the GIMC controller design, the robustness controller Q is designed to tolerate sensor faults as presented in [9]. In this way, sensor

faults are modelled by uncertainty in the output signal. This uncertainty representation can also be viewed as output multiplicative uncertainty. Finally, the performance of the three controllers K_0, K_∞ and GIMC are investigated. In this feedback configuration, there are two sensor measurements q_2 and q_4 (Axes 2 and 4). We consider the case when there is a sensor outage of Axis 2, *i.e.*,

$$\hat{q}_2(t) = \begin{cases} q_2(t), & t < t_0 \\ 0, & t \geqslant t_0 \end{cases}$$

where $\hat{q}_2(t)$ represents the measurement, $q_2(t)$ the true reading and t_0 the failure time. Thus, the simulation of the response to a square wave reference signal is computed with sensor fault in Axis 2 (q_2) at $t_0 = 8$ seconds as shown in Fig. 20.

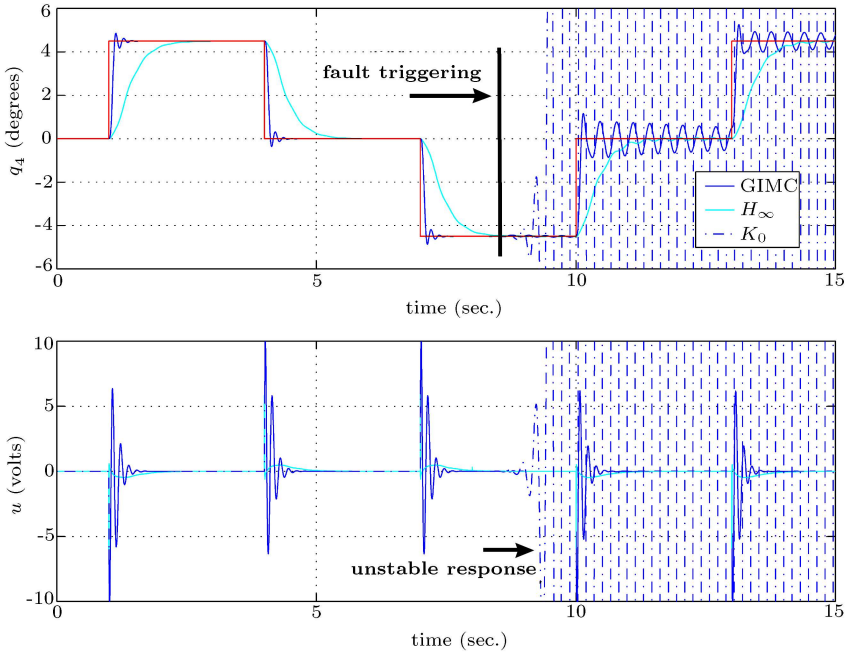

Fig. 20 Simulation with sensor fault at 8 sec.

From these plots, it is seen that the system with the nominal controller becomes unstable in the event of sensor fault. On the other hand, the systems with H_∞ and GIMC controllers remain stable. It can also be seen that the system response with the H_∞ controller is not clearly affected by the sensor fault, but the drawback is its slow response. As expected, the system with the GIMC controller keeps the performance of the nominal controller in the case of no fault, but in the case of fault, it still maintains stability with reasonable tracking.

In addition, these controllers are also tested experimentally. The responses to a square wave command signal (without fault) are shown in Fig. 21. The results present a peculiar behavior of the experimental configuration. While the rotor is spinning, the control signal applies an input voltage to motor #2 in order to rotate this gimbal, which produces a corresponding angular velocity in the gimbal #4 (q_4) direction. But due to friction mainly, small displacements of gimbal #2 (q_2) do not produce any motion in Axis 4. This behavior could be characterized by a dead-zone nonlinearity, but it is more complicated than that. Because, it is not coming from the dc-motor characteristics, instead it is related to interactions among gyroscope components. Consequently, the H_∞ controller response is drastically affected, since almost no movement in the Axis 4 direction is detected, producing a useless controller.

Meanwhile, the experimental response of the nominal controller K_0 is not much different from the simulation due to the high gain of this controller. On the other hand, the response with the GIMC controller is affected since there is large error between the model and true system. Nevertheless, the system with this controller still maintains good tracking.

Finally, the experimental response with fault in Axis 2 (q_2) sensor is tested. The fault is pro-

grammed at 2.2 seconds, *i.e.* the reading from that sensor is switched off after 2.2 seconds. No external disturbances are considered during testing. The results are shown in Fig. 22. The plot shows how the nominal controller K_0 immediately produces an unstable response, as predicted by simulation. Now, the real advantage of the GIMC architecture is obvious: even in the case of sensor fault (outage) the tracking capabilities are not significantly affected. After the sensor fault, q tries to compensate the nominal control signal $\hat{u}$ to preserve stability and to keep the tracking response.

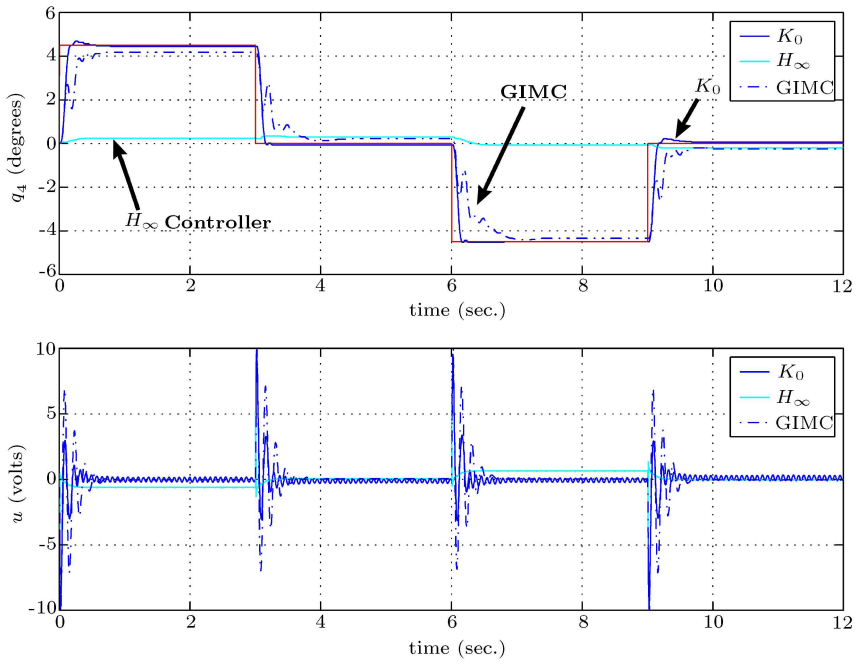

Fig. 21 Experimental responses without fault

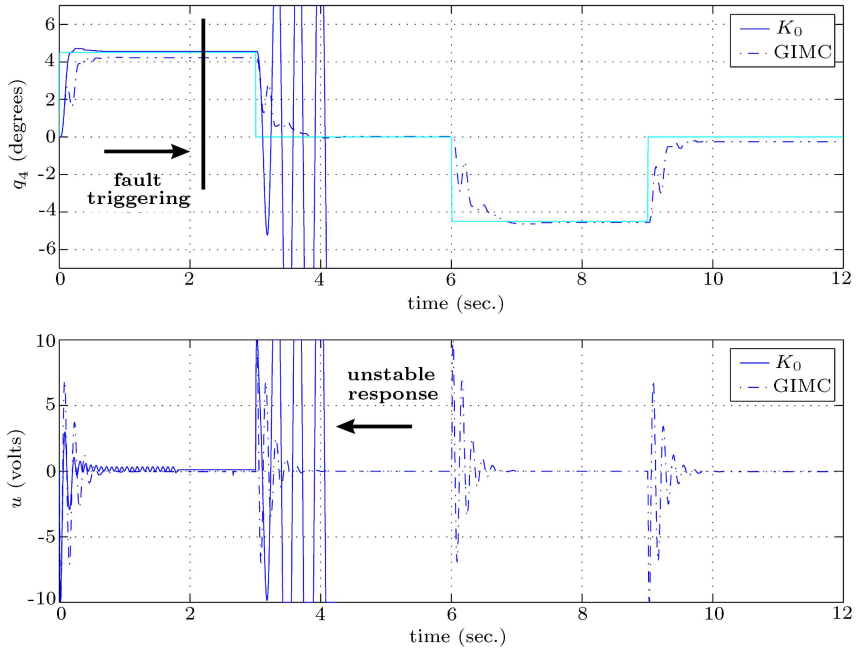

Fig. 22 Experimental responses with sensor fault at 2.2 sec.

Now, the idea proposed in Fig. 6 is followed. Thus, the robustness loop is switched on only in the case of a sensor failure. The failure condition is then detected by monitoring the signal r (residual). However, it is needed to choose a strategy to detect a sensor failure from the residual r. The following simple approach is chosen since external disturbances are not considered, check the standard behavior of this signal for no-failure case and set a threshold value such that if r goes above it the signal q is activated. The approach taken is by no means the most efficient way to detect the sensor failure, specially if external disturbances are considered. Other approaches like monitoring the statistics of r could lead to a more efficient detection. However, only the overall application is intended to be illustrated here. Nevertheless, if external disturbances are considered to influence the system, a detection strategy based on the norm of a weighted residual $\hat{r}$ over a finite period of time T [15] can be adopted, *i.e.*

$$J = \|\hat{r}(t)\|_{2,t,T} = \sqrt{\int_{t-T}^{t} \hat{r}^{\mathrm{T}}(\tau)\hat{r}(\tau)\mathrm{d}\tau} > J_{th}$$

where $\hat{r}(s) = R(s)[\tilde{N}(s)u(s) - \tilde{M}(s)y(s)]$, J_{th} is a threshold value to prevent false triggering, and $R(s)$ is a filter chosen to maximize the sensitivity to faults and minimize the effect of disturbances[16].

An important issue concerning the GIMC fault-tolerant structure of Fig. 6, is the possible delay in the failure detection. Since the compensation signal q is added after the failure is detected, the detection delay will have a big impact in the overall performance and stability. If this delay is too large, the performance will be dramatically affected and even the system can become unstable. In order to analyze this behavior, simulation was carried out assuming a failure in Axis 2 (q_2) sensor at 8 seconds and a detection delay of 0.35 seconds. The response is presented in Fig. 23, and it can be compared with Fig. 20 for the no-delay case. Therefore, it can be seen that the delay affects the output performance since the output became oscillatory after the fault is presented. Once the failure is detected the control signal is compensated but still some oscillation is observed. For a delay > 0.5 sec. the system cannot be stabilized anymore. Obviously, there is a strong relation among the size of the maximum delay allowable, the size of the saturation in the control signal, and the speed of response of the nominal controller. Thus, further analysis must be performed to obtain a measure of this maximum delay.

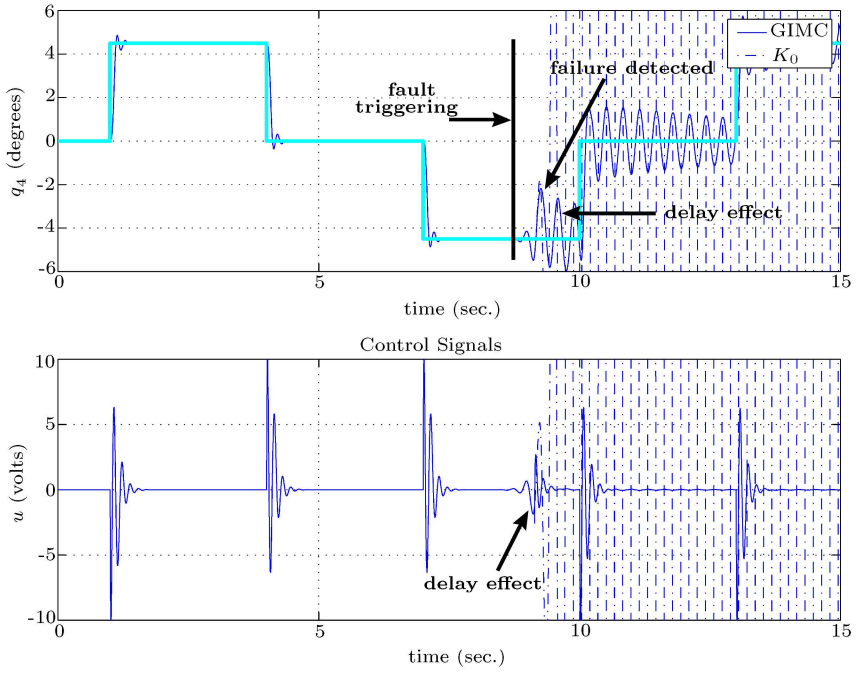

Fig. 23 Simulation with sensor fault at 8 sec. and delay of 0.35 sec. in detection

The fault-tolerant approach is tested in the experimental setup with failure of Axis 2 (q_2), sensor outage, after 6 sec as shown in Fig. 24. From this plot, it is clear that the controller is able to stabilize the system and achieve good performance even after the failure. Thus, the performance of the GIMC architecture is drastically improved since there is no sacrifice of performance for robustness before the fault.

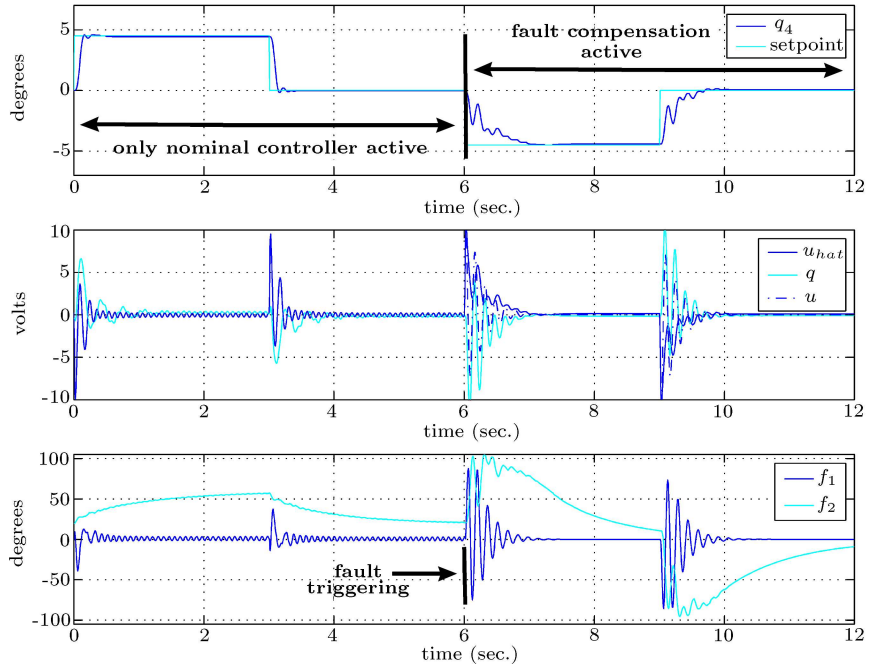

Fig. 24 Experimental responses: seitching on the robustness signal q after detecting sensor failure (6 sec.)

5 Conclusions

We have shown through two simple examples the effectiveness of the GIMC architecture for robust control and fault tolerant control. The price for achieving such a high performance and robust control is the complexity of the controller. In that regard, controller approximation method may be applied as suggested in [9]. Some detailed discussions of GIMC for fault tolerant control are given in [11]. Finally, we should point out the principle of GIMC can be generalized to nonlinear case easily in state space.

References

1 Chen J. Sensitivity integral relations and design trade-offs in linear multivariable feedback systems, *IEEE Transactions on Automatic Control*, 1995, **40**(10): 1700∼1716
2 Freudenberg J S, Looze D P. Frequency domain properties of scalar and multivariable feedback systems, In: Lecture Notes in Control and Information Science, Vol.104, Springer-Verlag, Berlin, 1988
3 Horowitz I M. Synthesis of Feedback Systems, Academic Press, London, 1963
4 Zhou K, Doyle J C, Essentials of Robust Control, Prentice Hall, Upper Saddle River, New Jersey, 1998
5 Zhou K, Doyle J C, Glover K. Robust and Optimal Control, Prentice Hall, Upper Saddle River, New Jersey, 1996
6 Balas G, Doyle J C, Glover K, Packard A, Smith R. μ-Analysis and Synthesis Toolbox, MUSYN Inc. and The MathWorks, Inc., 1991
7 Dahleh M, Diaz-Bobillo I J. Control of Uncertain Systems: A Linear Programming Approach, Prentice Hall, 1995
8 Doyle J C, Glover K, Khargonekar P P, Francis B A. State-space solutions to standard $\mathcal{H}_\infty$ and H_∞ control problems, *IEEE Transactions on Automatic Control*, 1989, **AC-34**(8): 831∼847
9 Zhou K, Ren Z. A New Controller Architecture for High Performance, Robust and Fault Tolerant Control, *IEEE Transactions on Automatic Control*, 2001, **46**(10): 1613∼1618

10 Campos-Delgado D U, Martinez Martinez S, Zhou K. Integrated fault tolerant scheme with disturbance feedforward, In: ACC 2004
11 Campos-Delgado D U, Zhou K. Reconfigurable fault tolerant control using GIMC structure, *IEEE Transactions on Automatic Control*, 2003, **48**(5): 832∼838
12 Marcos A, Ganguli S, Balas G. New strategies for fault tolerant control and fault diagnostic, In: 5$^{\text{th}}$ IFAC Symposium on Fault Detection, Supervision and Safety of Technical Processes (SAFEPROCESS'03), Washington, D.C., 2003
13 Chen J, Patton R J. Robust Model-Based Fault Diagnosis for Dynamic Systems, Kluwer Academic Publishers, 1999
14 Morari M, Zafiriou E. Robust Process Control. Prentice Hall, Englewood Cliffs, New Jersey, 1989
15 Ye H, Ding S X, Wang G. Integrated design for fault detection systems in time-frequency domain, *IEEE Transactions on Automatic Control*, 2002, **47**(2): 384∼390
16 Ding X, Guo L, Frank P M. A frequency domain approach to fault detection of uncertain dynamic systems, In: Proceedings IEEE Conference Decision Control, San Antonio, Texas, 1993, 1722∼1727

Kemin Zhou Received bachelor (1982) from Beijing University of Aeronautics and Astronautics, P.R.China, master (1986) and Ph.D. (1988) degrees both from University of Minnesota. He was a Research Fellow and Lecturer at California Institute of Technology from 1988 to 1990. Since 1990, he has been with the Department of Electrical and Computer Engineering, Louisiana State University. He was promoted to Associate Professor in 1996 and Full Professor in 2000. He is currently the Chair and the holder of the Voorhies Distinguished Professorship in Electrical Engineering. He is the leading author of two of the most popular books in the field: Robust and Optimal Control (Prentice Hall, 1995), which has been used worldwide as graduate textbook and research references and has been translated into Japanese (1997) and Chinese (2002), and Essentials of Robust Control (Prentice Hall, 1997). He is currently an Associate Editor of Automatica, Systems and Control Letters, Journal of System Sciences and Complexity, and Journal of Control Theory and Applications. He was also an Associate Editor of IEEE Transactions on Automatic Control and SIAM Journal on Control and Optimization. He has given numerous invited lectures and seminars around world. He was a member of international program committee for dozens of international conferences and holds several visiting positions around world. He received two book awards from the College of Engineering at LSU. He was named the Oskar R. Menton Endowed Professor in Electrical Engineering in 1998. He was given a certificate of special congressional recognition in 2003, recognition for outstanding accomplishments and contributions to Louisiana State University by the House of Representatives of the Louisiana Legislature in 2004, received outstanding young investigator award from Natural Science Foundation of China in 2004. He was elected to IEEE Fellow in 2003 for contributions to the robust control system theory and applications. His current research interests include fault diagnosis and fault tolerant control, control of combustion systems, robust and H-infinity control, probabilistic control theory, model and controller approximations, model identification, and some aspects of wireless communication. His work has been cited more than 2,200 times according to Science Citation Index. His research has been sponsored by AFOSR, ARO, LEQSF, NASA, and NSF.